RESEARCH ARTICLE

INTERNATIONAL RESEARCH JOURNAL OF MULTIDISCIPLINARY TECHNOVATION

Asian Research Association

DOI: 10.54392/irjmt25610

Comprehensive Analysis of Structural and Magnetic Properties of $Mn_2CoFeGe_2$ Double Half-Heusler Alloy

T. Naaraayanan [a, b, *], Prakash Bongurala [b], M. Saroja [a], M. Venkatachalam [a]

[a] Department of Electronics, Research and Development Centre, Erode Arts and Science College (Autonomous), Erode-638009, India.

[b] Department of Physics, Indian Institute of Technology Hyderabad, Hyderabad - 502 284, India.

* Corresponding Author Email: naaraayanan.t@phy.iith.ac.in

DOI: https://doi.org/10.54392/irjmt25610

Received: 10-09-2025; Revised: 28-10-2025; Accepted: 05-11-2025; Published: 10-11-2025

Abstract: Heusler alloys have unusual properties, making them highly interesting for evaluation. This study focuses on the double half-Heusler $Mn_2CoFeGe_2$, analyzing its crystal structure and magnetic properties. The prepared alloy was analysed through X-ray diffraction to study its structural features. The material's morphology was examined using scanning electron microscopy. Simultaneously, the elemental constituent proportions of $Mn_2CoFeGe_2$ were confirmed using energy-dispersive X-ray spectroscopy (EDS) analysis, which verifies that the elements are present in a 2:1:1:2 atomic ratio. Interestingly, the saturation magnetization slightly decreases from 60 emu/g at 5 K to 57 emu/g at 150 K. The measured g-value of the alloy is greater than 2. The $Mn_2CoFeGe_2$ alloy behaves like a semiconductor based on UV measurements. Therefore, the use of this alloy in the new technologies seems reasonable.

Keywords: Double half-Heusler alloy, $Mn_2CoFeGe_2$, Magnetic properties, Electron Spin Resonance, Raman spectroscopy

1. Introduction

Heusler alloys are part of a broad and adaptable group of intermetallic compounds. These alloys can be found in various configurations, including half-Heusler (X_1Y_1Z), full-Heusler ($X_2Y_1Z_1$), inverse Heusler, and other more complex binary and quaternary systems [1]. Z in these alloys is usually a main group element, and X, Y are typically transition metals. Heusler alloys have a broad profile of functional properties. These properties have made it a promising candidate for various uses in sensors, thermoelectric, magnetic shape memory devices, energy conversion, and magnetic refrigeration [2-10], even experimental investigations [11-13]. Their unique magnetic properties, they have been considered as potential candidates in spintronic and magneto-sensing technologies [14]. Nonetheless, dimensional stability is limited due to high thermal expansion. To mitigate this, mechanical modification [15] is employed. Screening based on modern machine learning techniques has been adopted to speed up the identification of new compositions with better thermal and structural stability [16].

An increasing subject is double half-Heusler (DHH) alloys. These compound alloys represent a new design concept to go beyond the intrinsic restrictions found in traditional half-Heusler systems. These are not simple doped or elementally substituted alloys, but rather are DHH alloys which have complex stoichiometric compositions giving rise to a variety of structures. There are triple phases, such as $X_2'X''Y_3Z_3$, quadruple phases like $X'_3X''Y_4Z_4$, and double quaternary phases, for example, compositions such as $X'X''Y_2Z_2$, $X_2Y'Y''Z_2$, and $X_2Y_2Z'Z''$. A great deal of work, in particular that of Anand *et al* [17] High Curie temperatures and use in magnetoelectronic devices make these materials promising. One of the common design strategies for such quaternary complex Heusler alloys is to combine two ternary phases, such as Co_2FeGe [18] and Co_2MnGe [19], to obtain the quaternary compound CoFeMnGe [20]. Some theoretical works predict that this alloy is probably a metal with a high Curie temperature. Recently, researchers have synthesized several quaternary alloys of the type CoFeMnX series, where X = Al, Si, Ga, Ge, further demonstrating the potential of such advanced Heusler systems [20, 21].

A novel compound $Mn_2CoFeGe_2$ was prepared and studied. This double half-Heusler alloy, which is a member of the well-known Heusler alloy family with various magnetic behaviors and promising technological applications, reveals great promise in the field of magnetism. In this regard, the indigenous doping approach in $Mn_2CoFeGe_2$ makes it an ideal candidate material for potential applications like thermoelectric

energy conversion, magnetocaloric effect (magnetic refrigeration), optoelectronics, and high-density data storage [22, 23]. Both the crystallographic and magnetic properties of $Mn_2CoFeGe_2$ are found to be heavily influenced by the substitution of Mn, Co, and Fe atoms, while Ge plays a crucial role in determining both cluster geometry, coordination environment, and thus chemical bonding within the alloy. The experimental study comprises a detailed structural characterization that was conducted using powder X-ray diffraction (XRD) and energy-dispersive X-ray spectroscopy (EDS or EDX). The morphology was characterized through Scanning Electron Microscopy (SEM). Magnetic properties were carefully examined using a Physical Property Measurement System (PPMS) and Electron Spin Resonance (ESR). Furthermore, UV–Vis–NIR was employed to analyze the optical absorbance spectra. The characteristic features associated with electronic excitations in the Raman spectra need to be determined.

2. Experimental Details

The $Mn_2CoFeGe_2$ double half-Heusler compound was melted using arc melting of the elemental components in the right stoichiometric ratio. High-purity Mn (99.99%), Fe (99.99%), Co (99.99%), and Ge (99.99%) were accurately weighed, placed in a copper crucible, and melted three to four times in an arc furnace under an argon atmosphere. To compensate for Mn volatilization during melting, an additional 3% Mn was included. Circulating cold water cooled the system, and multiple melting improved the alloys homogeneity, resulting in a final weight loss of less than 1%.

To further enhance the homogeneity, the melted sample in the arc was finally sealed into a quartz ampoule and then heated. After annealing at 1000 °C for six hours in a tube furnace, the sample was allowed to cool on its own to ambient temperature before it was taken out for analysis. Powder samples were subjected to Cu-Kα radiation (1.5406 Å) to capture X-ray diffraction patterns at ambient temperature (Rigaku Smart Lab, Japan). With a JEOL JIB 4700 FIB-SEM in EDS mode and collecting EDS data, we quantified the sample composition with scanning electron microscopy. The investigation of magnetic properties is performed with the PPMS (Dynacool Quantum Design, USA) with an applied magnetic field ranging from −7 to +7 Tesla (T), and with the temperature swept from 5 K to 300 K.

A JEOL (JES FA200) spectrometer was utilized to capture the ESR data at an applied frequency of X-band, with the magnetic field varying from 0 to 800 mT. Additionally, a PerkinElmer Lambda 1050 UV-Vis spectrophotometer was employed to assess the optical absorbance spectra were recorded at ambient temperature, with wavelengths measured between 200 and 800 nm.

The Raman spectra of the samples were captured with a custom-made optical system. This enabled accurate characterization of the materials, which showed clear peaks corresponding to their molecular vibrations. An Andor Kymera 328i spectrometer coupled with an Oxford Instruments Newton 920 CCD camera was the core of the setup, along with an inverted microscope (Nikon Ti2U, Nikon). The samples were excited using a 60× objective (N) via a glass substrate. The 594 nm laser source used is an OBIS 594LX model from Coherent with an objective lens of power 5 mW to detect scattered light via the same objective (NA = 0.7). Each spectrum was recorded using a 60-second interval and repeated three times, with a notch filter positioned prior to the spectrometer to eliminate Rayleigh scattering.

3. Results and Discussion

3.1. Structural Analysis

The XRD pattern of the prepared $Mn_2CoFeGe_2$ powder confirms its crystalline nature and indicates a combination of two distinct crystalline phases. Phase identification was carried out with X'Pert High Score Plus (HSP) software, and the fitted data are presented in Figure 1. The fitted results indicated that the synthesized $Mn_2CoFeGe_2$ comprises a cubic and an orthorhombic crystal structure. The primary phase (83%) corresponds to an orthorhombic structure with the *P-nma* space group as indicated by reference code 96-210-6530. The secondary phase (17%) is identified as a cubic structure with space group *Im-3m* according to reference code 96-901-3485. A literature by E. Yüzüak *et. al.* studied a similar $CoMn_{0:9}Fe_{0:1}Ge$ alloy, and showed a secondary phase [24]. This polymorphism may affect the material properties by potentially combining characteristics from both the orthorhombic and cubic phases. The lattice parameters are found to be a = 5.283270 Å, b = 4.095393 Å, and c = 7.112414 Å for the orthorhombic structure, a = 2.898657 Å, b = 2.898657 Å, and c = 2.898657Å for the cubic structure. Studies on related MnCoGe-based alloys reveal that structural transitions frequently occur between orthorhombic (low symmetry) and hexagonal or cubic (higher symmetry) phases, often accompanied by magnetic phase transitions. These transitions can be first order and strongly coupled to magnetism, resulting in notable magneto-structural effects. Adjustment of synthesis conditions, such as annealing temperature, annealing time, and cooling rate. High-temperature annealing for long duration followed by slow cooling is expected to promote single-phase formation, while rapid cooling or insufficient annealing may lead to the formation of multiple phases or structural disorder [25], [26]. The Structural strain was calculated by the Williamson-Hall plot of XRD data and found that 2.88x 10-4.

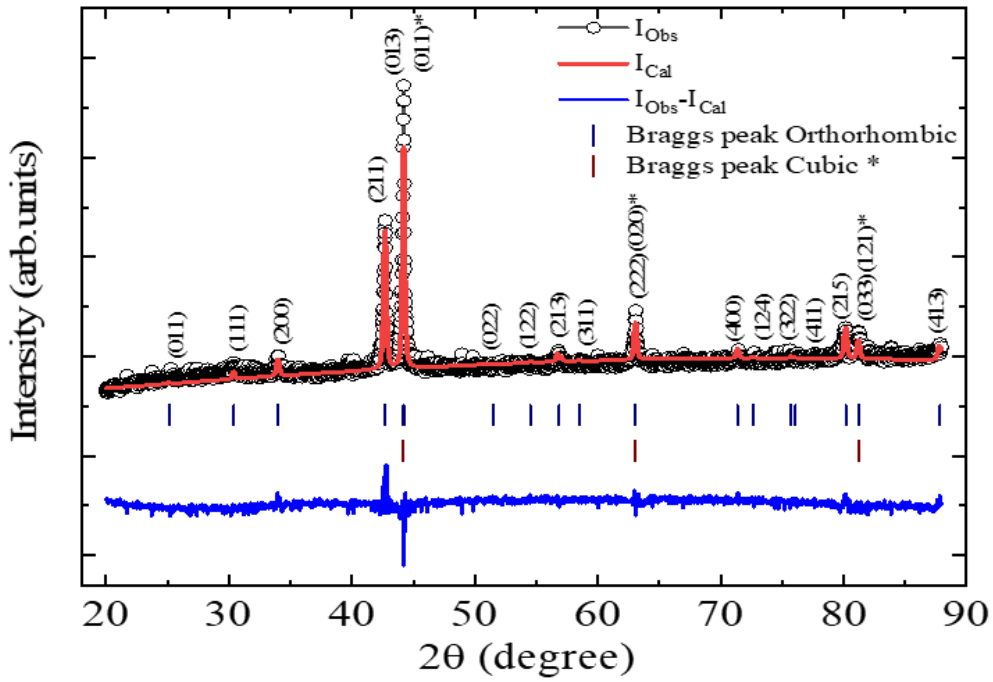

Figure 1. X-ray diffraction patterns of the $Mn_2CoFeGe_2$ alloy obtained at ambient temperature: The plot displays the experimental data (black), fitted curve (red), difference plot (blue), and Bragg peak positions (vertical lines).

3.2 Morphological Analysis

The synthesized $Mn_2CoFeGe_2$ alloy powders are shown in Figure 2, which reveals their morphology and elemental composition. The synthesized powder sample $Mn_2CoFeGe_2$ alloy possesses a granular nature, as evident from the SEM image in Figure 2(a).

EDS was used to check the chemical composition of $Mn_2CoFeGe_2$, and the findings in Figure 2(b) match the nominal composition. Which was discovered to fit the nominal composition. The volume particles homogeneous of Mn, Fe, Co, and Ge were discovered through X-ray element mapping; no obvious inhomogeneities were discovered. The atomic percentage ratio of the composition of the $Mn_2CoFeGe_2$ double half-Heusler alloy was identified through EDS, and the findings are presented in Table 1. The atomic percentage ratio of the composition being 2:1:1:2 agrees with the values anticipated from the findings.

3.3 UV Spectra Analysis

The optical behavior of the $Mn_2CoFeGe_2$ double half-Heusler alloy was studied through UV–visible spectroscopy in the wavelength region 250-800 nm. The absorption spectrum, shown in Figure 3 alongside the corresponding graph of hv (energy) versus $(\alpha hv)^{1/2}$, reveals that the $Mn_2CoFeGe_2$ alloy has a wide absorption peak near 320 nm. By extrapolating the linear section of the Tauc plot shown in the plot inside sub-Figure 3, the optical band gap (E_g) is found to be 1.07 eV, confirming its semiconducting nature. Double half-Heusler alloys possess mostly semiconducting character with band gaps of 0.2–1.0 eV, depending on composition, atomic ordering, and phase stability. These gaps position the absorption edge between the infrared and visible parts of the spectrum, with higher-gap compositions reaching into the near-UV [27-29]. The Double half-Heusler alloys show semiconducting behaviour with similar band gap values in the literature [30-31].

3.4 Magnetic Properties

The magnetic hysteresis (M–H) loops corresponding to the $Mn_2CoFeGe_2$ sample in the −7 T to +7 T magnetic field range at 5 K, 150 K, and 300 K, corresponding to the ferromagnetic, near-transition, and paramagnetic regimes, respectively, as shown in Figure 4 (a). Magnetic characteristics, including saturation magnetization (M_s), magnetic coercivity (H_c), and remanence magnetization (M_r), were derived from the M-H loops. The $Mn_2CoFeGe_2$ sample exhibits a saturation magnetization of approximately 60 emu/g at 5 K and 57 emu/g at 150 K in the presence of an applied field of 4 kOe. The increase in Ms at lower temperatures arises from the thermal ordering of magnetic moments along the applied field. The M–H loop measured at 300 K displays paramagnetic behavior, consistent with the sample's Curie temperature (Tc~250K).

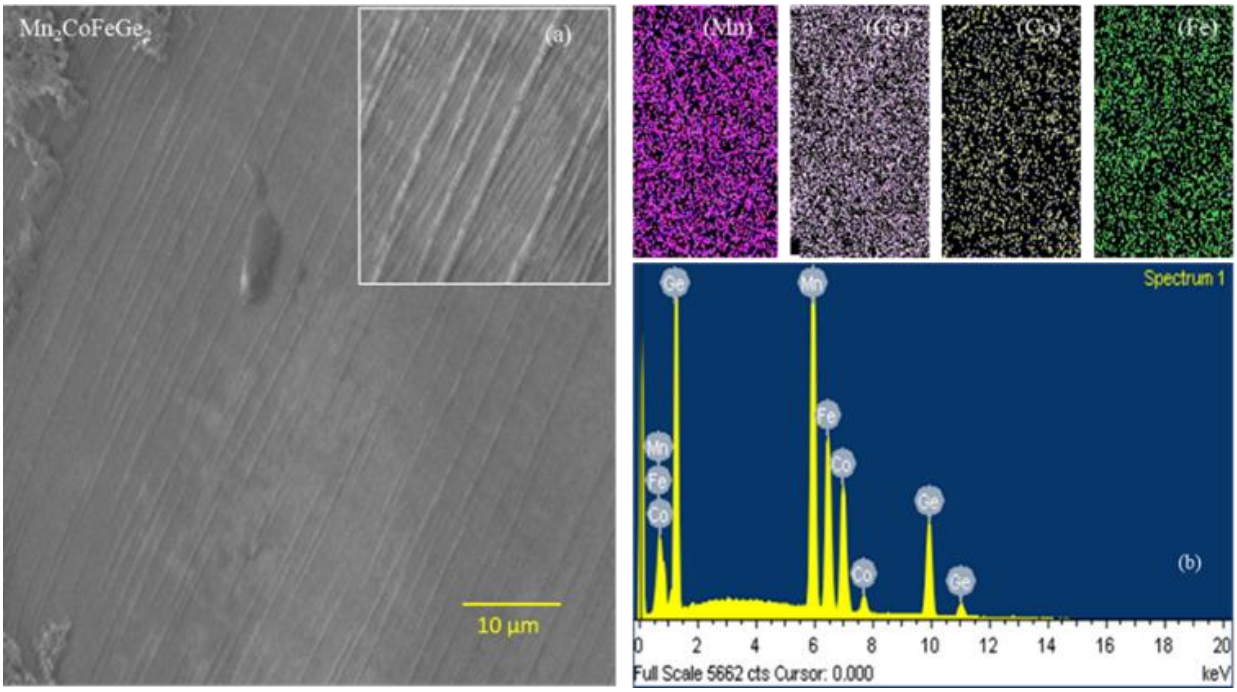

Figure 2. (a) High-Resolution SEM Images of the Material. (b) Elemental mapping and EDS pattern of the $Mn_2CoFeGe_2$ alloy.

Table 1. Composition ratio for $Mn_2CoFeGe_2$ double half-Heusler alloy.

DHH alloy ($Mn_2CoFeGe_2$)	Manganese (Mn)		Cobalt (Co)		Iron (Fe)		Germanium (Ge)	
	Weight (%)	Atomic (%)	Weight (%)	Atomic (%)	Weight (%)	Atomic (%)	Weight (%)	Atomic (%)
Spectrum 1	29.23	32.77	16.14	16.87	15.71	17.33	38.92	33.03
Composition Ratio	2 :		1 :		1 :		2	

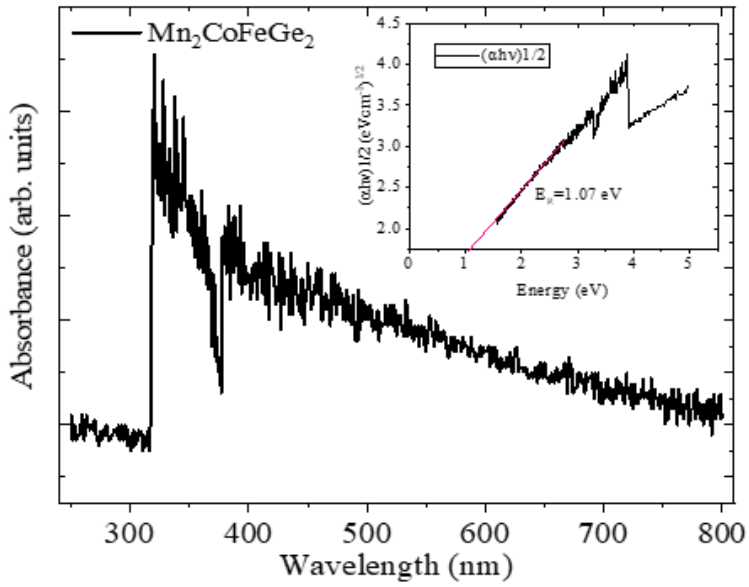

Figure 3. UV absorption spectrum and tau plot of $Mn_2CoFeGe_2$ double half-Heusler alloy

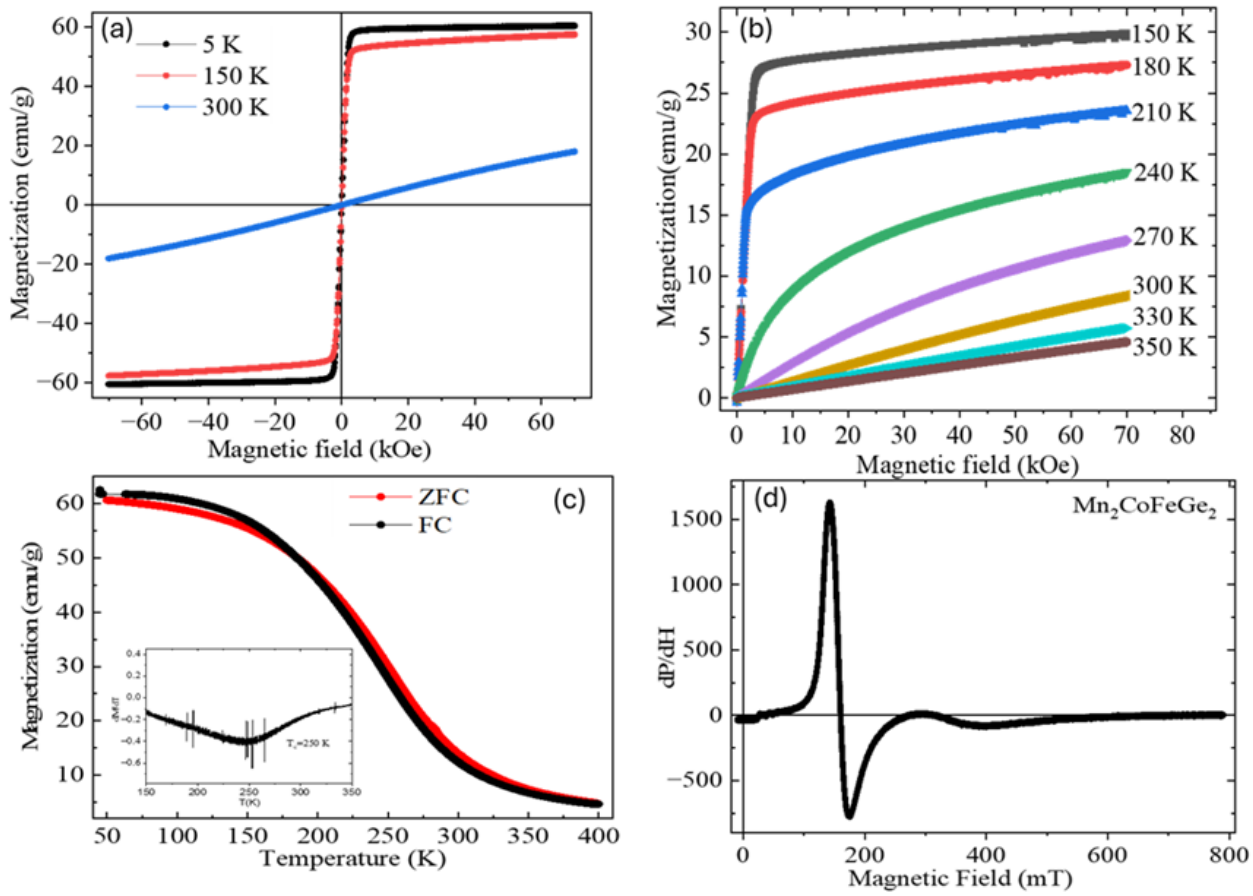

Figure 4. (a) The field dependence of magnetization was measured at 5 K, 150 K, and 300 K. (b) Magnetization isotherms were recorded at various temperatures. (c) Temperature-dependent magnetization was measured under FC and ZFC conditions. (d) Electron spin resonance spectra of the $Mn_2CoFeGe_2$ alloy.

There is a drastic decrease in the remanent magnetization (M_r), which drops from 1.109emu/g at 150 K to 0.283 emu/g at 5 K. The H_c values found that 30 Oe and 64 Oe at 150 K and 5 K respectively. These findings establish that the $Mn_2CoFeGe_2$ alloy exhibits soft ferromagnetic characteristics.

Figure 4(c) illustrates that the temperature-dependent magnetization (M–T) of the $Mn_2CoFeGe_2$ double half-Heusler sample exhibits a field-induced transition from a high-temperature paramagnetic state to a low-temperature ferromagnetic state below Tc. measurements were performed in a field of 5 kOe with both zero-field-cooled (ZFC) and field-cooled (FC) procedures. The measurements were carried out in the presence of an external magnetic field of 5 kOe using ZFC and FC processes. The ZFC and FC curves almost entirely collapse on top of each other in the temperature range, making them nearly inseparable. However, the curves show a sharp jump of magnetization at 250 K and some weak bifurcation at low temperature. The Curie temperature was found to be 250 K from dM/dT plot, shown in the insert of Figure 4c. The Tc value of the prepared material matching with similar materials in the literature [32, 33].

Isothermal magnetization (M–H) curves of $Mn_2CoFeGe_2$ were measured from 150 to 350 K at 30 K intervals, as presented in Figure 4(b). For the 350–300 K range, the M–H profiles show a linear dependence on applied field, typical of paramagnetic behavior. Between 270 and 240 K, there is a transitional regime from the curves, whereas from 240–150 K, as the temperature falls from 350K to 150K, $Mn_2CoFeGe_2$ shifts from being paramagnetic to ferromagnetic, with a distinct intermediate region serving as a transitional phase. Magnetization strength and nature are thus extremely temperature-dependent, with ferromagnetic order and increased magnetocaloric behavior seen at lower temperatures. Similar Heusler alloys (like Mn_2FeGe and Fe_2MnGe) also show ferromagnetic ordering with comparable or higher saturation magnetization values (up to ~5.1 μB/f.u. for Fe-substituted samples), and Curie temperatures ranging from about 200 K to above 400 K [34]. Other Co/Fe-doped Mn-rich Heusler alloys, like CoFeMnGe or Mn–Ni–Ga-based analogs, exhibit intense ferromagnetism and magnetocaloric effects near ambient temperature, occasionally with greater magnetic moments (e.g., Co_2FeGe: 6.1 μB/f.u., Fe_2MnGe: 5 μB/f.u.) and similar entropy changes for magnetocaloric devices [35].

3.5. Electron Spin Resonance Study

ESR measurements for the $Mn_2CoFeGe_2$ double half-Heusler alloy were conducted at ambient temperature across a magnetic field range of 0–800 mT. The derivative spectra of microwave absorption for the applied magnetic field are presented in Figure 4(d). The analysis yielded a g-factor of 4.17, a resonance field (H_r) of 160 mT, a peak-to-peak linewidth (ΔH_{pp}) of 31.65 mT, and an absorption positive and negative intensity ratio ($\frac{A}{B}$) of 2.09. As shown in Figure 4(d), the ESR signal exhibits characteristic variations with the applied magnetic field, reflecting the alloys non-magnetic matrix. The $Mn_2CoFeGe_2$ alloy displays magnetic spin resonance with distinct positive and negative peaks as the field is varied, a behavior arising from unpaired electrons localized in the ferrite phase of the composite, which are primarily responsible for the ESR response.

The equation was used to calculate the g-factor [36].

$$g = \frac{h\nu}{\mu_B H_r}$$

Here h is Planck's constant, μB is the Bohr magneton, v is the microwave frequency (in Hz), and Hr is the resonance field (in Tesla). The g-value found is more than 2; the reason could be the substantial orbital contribution to the magnetic moment, compared with the literature [37], [38]. In Heusler alloys, transition metals such as Co, Fe, and Mn retain partial orbital angular momentum due to crystal-field and spin–orbit coupling effects. The ($\frac{A}{B}$) ratio measures approximately 2. For free electrons, the ratio ($\frac{A}{B}$) is approximately equal to one. However, in the present $Mn_2CoFeGe_2$ alloy, this ratio is greater than unity because of the spin resonance high spin coupling to other spins. The relative intensities of absorption around 2 are sensitive to the diagnosis of magnetic phase composition, spin dynamics, and electronic structure. These are known to exist in several Heusler alloy systems, such as Co_2MnSi, Ni-Mn-In-Si, and Mn-Co-Fe-Ge compounds, because these have been demonstrated by systematic ESR and magnetic resonance studies [39, 40].

3.6. Raman Spectroscopy Analysis

The Raman spectrum of $Mn_2CoFeGe_2$ at ambient temperature exhibits a Raman shift within the range of values from 550 cm^{-1} to 700 cm^{-1}, in the prepared alloy shows the Raman peak is at 630 cm^{-1}, as presented in Figure 5. There are very few experimental Raman spectra that have been reported for Heusler alloys [41, 42] For instance, Bera *et al.* [43] A Raman peak was observed at 645 cm^{-1} for the NiFeMnSn sample. Attributed to crystal field excitations, which significantly enhanced the vibrational characteristics of Heusler alloys. Here, anticipates the observed Raman peak due to atom vibrations in the orthorhombic structure. Although most Heusler alloys exhibit either metallic or semi-metallic properties.

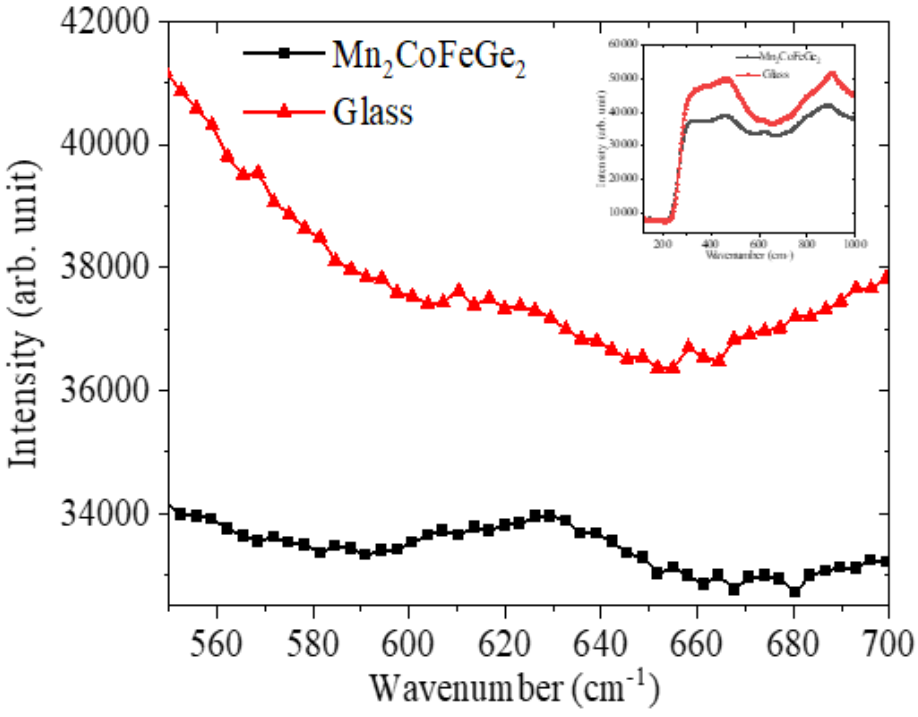

Figure 5. Ambient temperature Raman spectrum of the sample.

4. Conclusions

A novel double half-Heusler alloy, $Mn_2CoFeGe_2$, was synthesized for the first time via arc melting. Here, its structure and magnetic properties have been studied and presented for the first time. X-ray diffraction experiments confirmed that the compound is orthorhombic (*P-nma*) and cubic (*Im-3m*) in nature. Energy-dispersive X-ray spectroscopy confirmed the elemental composition of the alloys, whereas scanning electron microscopy ascertained a well-homogenized microstructure. Magnetic measurements from 300 K to 5 K revealed a clear transition from paramagnetic to ferromagnetic behavior. ESR measured the g-value of the alloy is greater than 2. The alloy behaves like a semiconductor based on UV measurements. These findings not only reveal significant detail regarding the crystal structure and magnetism of $Mn_2CoFeGe_2$ but also create a solid platform for further work. Due to its magnetically tunable nature, this material shows immense potential for use in magnetocaloric applications.

References

[1] S. Tavares, K. Yang, M.A. Meyers, Heusler alloys: Past, properties, new alloys, and prospects. Progress in Materials Science, 132, (2023) 101017. https://doi.org/10.1016/j.pmatsci.2022.101017

[2] Y. El Krimi, R. Masrour, Cobalt-based full Heusler compounds Co_2FeZ (Z = Al, Si, and Ga): A comprehensive study of competition between XA and L21atomic ordering with ab initio calculation. Materials Science and Engineering: B, 284, (2022) 115906. https://doi.org/10.1016/j.mseb.2022.115906

[3] M.Y. Raïâ, R. Masrour, M. Hamedoun, J. Kharbach, A. Rezzouk, A. Hourmatallah, N. Benzakour, K.J.S.S.C. Bouslykhane, Effect of L21 and XA ordering on structural, martensitic, electronic, magnetic, elastic, thermal and thermoelectric properties of Co_2FeGe Heusler alloys. Solid State Communications, 355, (2022) 114932. https://doi.org/10.1016/j.ssc.2022.114932

[4] S.S. Essaoud, A.S. Jbara, First-principles calculation of magnetic, structural, dynamic, electronic, elastic, thermodynamic and thermoelectric properties of Co_2ZrZ (Z = Al, Si) Heusler alloys. Journal of Magnetism and Magnetic Materials, 531, (2021) 167984. https://doi.org/10.1016/j.jmmm.2021.167984

[5] A. Telfah, S. Sâad Essaoud, H. Baaziz, Z. Charifi, A.M. Alsaad, M.J.A. Ahmad, R. Hergenröder, R. Sabirianov, Density Functional Theory Investigation of Physical Properties of KCrZ (Z = S, Se, Te) Half-Heusler Alloys. Physica Status Solidi (b), 258(10), (2021) 2100039. https://doi.org/10.1002/pssb.202100039

[6] M.Y. Raïâ, R. Masrour, M. Hamedoun, J. Kharbach, A. Rezzouk, A. Hourmatallah, N. Benzakour, K. Bouslykhane, Diluted effect on the structural, magnetic, electronic, thermodynamic, optical and thermoelectric properties of the Heusler alloys $Co_2Fe_{1-x}Ti_xGa$: GGA and GGA + U Approaches. Optical and Quantum Electronics, 55(2), (2023) 140. https://doi.org/10.1007/s11082-022-04348-6

[7] A. Ezaier, R. Masrour, M. Hamedoun, J. Kharbach, A. Rezzouk, A. Hourmatallah, N. Benzakour, K. Bouslykhane, First principal study of structural, electronic, magnetic, thermodynamic, optical and thermoelectric properties of $Nd(Co_{1-x}Fe_x)_2$ (x=0 to 1). Journal of Physics and Chemistry of Solids, 176, (2023) 111194. https://doi.org/10.1016/j.jpcs.2022.111194

[8] I.A. Elkoua, R. Masrour, Structural, thermodynamics, optical, electronic, magnetic and thermoelectric properties of Heusler Ni_2MnGa: An ab initio calculations. Optical and Quantum Electronics, 54(10), (2022) 667. https://doi.org/10.1007/s11082-022-03999-9

[9] M.L. Belkhir, A. Gueddouh, F. Faid, M. Rougab, The Structural, Electronic, Magnetic, Mechanical, and Lattice Dynamical Properties of the Novel Full-Heusler Alloys Mn_2HfX (*X* = Si and Ge): Ab Initio Study. Journal of Superconductivity and Novel Magnetism, 36(1), (2023) 131–146. https://doi.org/10.1007/s10948-022-06431-1

[10] P.Y. Huang, Z.G. Zheng, S. Da, Z.G. Qiu, G. Wang, D.C. Zeng, Large magnetocaloric effect and negative thermal expansion of Mn-Ni-Si-Fe-Co-Ge high-entropy alloys. Journal of Alloys and Compounds, 1007, (2024) 176394. https://doi.org/10.1016/j.jallcom.2024.176394

[11] [11] M. Kratochvílová, D. Král, M. Dušek, J. Valenta, R.H. Colman, O. Heczko, M. Veis, Fe_2MnSn - Experimental quest for predicted Heusler alloy. Journal of Magnetism and Magnetic Materials, 501, (2020) 166426. https://doi.org/10.1016/j.jmmm.2020.166426

[12] S. Fabbrici, F. Cugini, F. Orlandi, N.S. Amadè, F. Casoli, D. Calestani, R. Cabassi, G. Cavazzini, L. Righi, M. Solzi, F. Albertini, Magnetocaloric properties at the austenitic Curie transition in Cu and Fe substituted Ni-Mn-In Heusler compounds. Journal of Alloys and Compounds, 899, (2022) 163249. https://doi.org/10.1016/j.jallcom.2021.163249

[13] F. Cugini, S. Chicco, F. Orlandi, G. Allodi, P. Bonfá, V. Vezzoni, O.N. Miroshkina, M.E. Gruner, L. Righi, S. Fabbrici, F. Albertini, Effective decoupling of ferromagnetic sublattices by frustration in Heusler alloys.

Physical Review B, 105(17), (2022) 174434. https://doi.org/10.1103/PhysRevB.105.174434

[14] A. Cheriet, K. Boudia, R. Hamdi, F. Sofrani, F. Khelfaoui, Computational characterization of structural, electronic, elastic and magnetic properties of double half-Heusler alloy Fe2MnCoGe2**.** Studies in Engineering and Exact Sciences, 5(2), (2024) e11737. https://doi.org/10.54021/seesv5n2-673

[15] C.H. Tsau, M.C. Tsai, W.L. Wang, Microstructures of FeCoNiMo and CrFeCoNiMo Alloys, and the Corrosion Properties in 1 M Nitric Acid and 1 M Sodium Chloride Solutions. Materials, 15(3), (2022) 888. https://doi.org/10.3390/ma15030888

[16] G. Vazquez, S. Chakravarty, R. Gurrola, R. Arróyave, A deep neural network regressor for phase constitution estimation in the high entropy alloy system Al-Co-Cr-Fe-Mn-Nb-Ni. npj Computational Materials, 9(1), (2023) 68. https://doi.org/10.1038/s41524-023-01021-8

[17] S. Anand, M. Wood, Y. Xia, C. Wolverton, G.J. Snyder, Double Half-Heuslers. Joule, 3(5), (2019) 1226–1238. https://doi.org/10.1016/j.joule.2019.04.003

[18] B. Balke, S. Wurmehl, G.H. Fecher, C. Felser, M. Alves, F. Bernardi, J. Morais, Structural characterization of the Co_2FeZ (Z=Al, Si, Ga, and Ge) Heusler compounds by x-ray diffraction and extended x-ray absorption fine structure spectroscopy. Applied Physics Letters, 90(17), (2007) 172501. https://doi.org/10.1063/1.2731314

[19] Y. Zhang, J. Sung, Y. Yin, Y.Y. Chang, N.V. Medhekar, S. Granville, H.S. Hsu, Giant temperature-independent ultraviolet circular dichroism in Co_2Mn X (X = Ga,Ge) Heusler magnetic thin films. Physical Review Applied, 24(3), (2025) 034052. https://doi.org/10.1103/h822-rw47

[20] V. Alijani, S. Ouardi, G.H. Fecher, J. Winterlik, S.S. Naghavi, X. Kozina, G. Stryganyuk, C. Felser, E. Ikenaga, Y. Yamashita, S. Ueda, Electronic, structural, and magnetic properties of the half-metallic ferromagnetic quaternary Heusler compounds CoFeMn Z (Z = Al , Ga, Si, Ge). Physical Review Applied, 84(22), (2011) 224416. https://doi.org/10.1103/PhysRevB.84.224416

[21] P. Klaer, B. Balke, V. Alijani, J. Winterlik, G.H. Fecher, C. Felser, H.J. Elmers, Element-specific magnetic moments and spin-resolved density of states in CoFeMn Z (Z = Al , Ga; Si, Ge). Physical Review B, 84(14), (2011) 144413. https://doi.org/10.1103/PhysRevB.84.144413

[22] H.A. Masri, M.S. Abu-Jafar, N.F.A. Mohammad, S.S. Essaoud, Extensive DFT study of FeMnCrGe quaternary Heusler alloy: structural, elastic, magnetic, optical and thermoelectric properties. Optical and Quantum Electronics, 57(2), (2025) 139. https://doi.org/10.1007/s11082-024-08029-4

[23] K. Berarma, S.S. Essaoud, A.A. Mousa, S.M. Azar, A.Y. Al-Reyahi, Opto-electronic, thermodynamic and charge carriers transport properties of Ta2 FeNiSn2 and Nb2 FeNiSn2 double half-Heusler alloys. Semiconductor Science and Technology, 37(5), (2022) 055013. https://doi.org/10.1088/1361-6641/ac612b

[24] E. Yüzüak, I. Dincer, Y. Elerman, I. Dumkow, B. Heger, S. Yuce Emre, Enhancement of magnetocaloric effect in $CoMn_{0.9}Fe_{0.1}$ Ge alloy. Journal of Alloys and Compounds, 641, (2015) 69–73. https://doi.org/10.1016/j.jallcom.2015.04.062

[25] X.Y. Wang, M. Li, Z.X. Wen, The Effect of the Cooling Rates on the Microstructure and High-Temperature Mechanical Properties of a Nickel-Based Single Crystal Superalloy. Materials, 13(19), (2020) 4256. https://doi.org/10.3390/ma13194256

[26] S. Ghosh, A. Nozariasbmarz, H. Lee, L. Raman, S. Sharma, R.B. Smriti, D. Mandal, Y. Zhang, S.K. Karan, N. Liu, J.L. Gray, High-entropy-driven half-Heusler alloys boost thermoelectric performance. Joule, 8(12), (2024) 3303–3312. https://doi.org/10.1016/j.joule.2024.08.008

[27] S.S. Beenaben, R. Sankararajan, S. Manickam, K. KlintonBrito, M. Prasath, MnNiSi Half-Heusler Alloy: Computational and experimental insights for energy harvesting and spintronic applications. Chemical Physics Impact, 10, (2025) 100891. https://doi.org/10.1016/j.chphi.2025.100891

[28] S. Saad Essaoud, S. Al Azar, A.A. Mousa, A.Y. Al-Reyahi, N. Al Aqtash, M.E. Ketfi, Insight into physical properties of lutetium-based double half-Heusler alloys $LuXCo_2Bi_2$ (X = V, Nb and Ta). Journal of Rare Earths, 43(1), (2025) 199–208. https://doi.org/10.1016/j.jre.2023.11.011

[29] C.O. Dias, J.R.D.M. Monteiro, L.S.D. Oliveira, P. Chaudhuri, S.M.D. Souza, D.M. Trichês, Combined Experimental and First Principles Study on Nanostructured NbFeSb Half-Heusler Alloy Synthesized by Mechanical Alloying. Materials Research, 26, (2023) e20220295. https://doi.org/10.1590/1980-5373-MR-2022-0295

[30] N.S. Soltanbek, N. Merali, N.E. Sagatov, F.U. Abuova, E. Elsts, A.U. Abuova, V. Khovaylo, T. Inerbaev, M. Konuhova, A.I. Popov, Ab Initio Investigation of the Stability, Electronic, Mechanical, and Transport Properties of New Double Half Heusler Alloys Ti_2Pt_2ZSb (Z = Al, Ga, In). Metals, 15(3), (2025) 329. https://doi.org/10.3390/met15030329

[31] S.A. Khandy, I. Islam, D.C. Gupta, R. Khenata, A. Laref, Lattice dynamics, mechanical stability

and electronic structure of Fe-based Heusler semiconductors. Scientific reports, 9(1), (2019) 1475. https://doi.org/10.1038/s41598-018-37740-y

[32] R. Boya, V. Yenugonda, E. Purushotham, J. Casey, S.K. Adpa, M. Chandra Sekhar, G. Nataraju, S.S. Samatham, A.K. Pathak, Weak first-order phase transition, exchange bias effect, and T − H phase diagram of $Mn_{0.75}Fe_{0.25}$ NiGe. Physical Review Materials, 8(11), (2024) 114411. https://doi.org/10.1103/PhysRevMaterials.8.114411

[33] J. Sharma, A.A. Coelho, K.G. Suresh, A. Alam, Martensitic and room-temperature magnetocaloric properties of Mn-rich Mn-Ni-Sn Heusler alloys: Experiment and theory. Physical Review B, 109(6), (2024) 064418. https://doi.org/10.1103/PhysRevB.109.064418

[34] A. Aryal, I. Dubenko, J. Zamora, J.S. Llamazares, C.F. Sánchez-Valdés, D. Mazumdar, S. Talapatra, S. Stadler, N. Ali, Synthesis, structural, and magnetic properties of Heusler-type $Mn_{2-x}Fe_{1+x}Ge$ ($0.0 \leq x \leq 1.0$) alloys. Journal of Magnetism and Magnetic Materials, 538, (2021) 168307. https://doi.org/10.1016/j.jmmm.2021.168307

[35] N. Tiwari, S. Mishra, S. Sarkar, S. Talapatra, M. Palit, M. Paliwal, A.K. Singh, C.S. Tiwary, Magnetocaloric effect in Mn-rich Heusler-derived alloys for room temperature-based applications. Journal of Materials Chemistry C, 13(21), (2005) 10789–10803. https://doi.org/10.1039/D4TC04242E

[36] X. Cao, L. Gu, Spindly cobalt ferrite nanocrystals: preparation, characterization and magnetic properties. Nanotechnology, 16(2), (2005) 180.https://doi.org/10.1088/0957-4484/16/2/002

[37] Ł. Dubiel, B. Cieniek, W. Maziarz, I. Stefaniuk, Electron Magnetic Resonance Study of $Ni_{50.2}Mn_{28.3}Ga_{21.5}$ Powders. Materials, 17(17), (2024) 4391. https://doi.org/10.3390/ma17174391

[38] A. Vovk, S.A. Bunyaev, P. Štrichovanec, N.R. Vovk, B. Postolnyi, A. Apolinario, J.A. Pardo, P.A. Algarabel, G.N. Kakazei, J.P. Araujo, Control of Structural and Magnetic Properties of Polycrystalline Co_2FeGe Films via Deposition and Annealing Temperatures. Nanomaterials, 11(5), (2021) 1229. https://doi.org/10.3390/nano11051229

[39] Y.S. Chen, J.G. Lin, I.S. Titov, A.B. Granovsky, Electron spin resonance probed competing states in NiMnInSi Heusler alloy. Journal of Magnetism and Magnetic Materials, 407, (2016) 365–368. https://doi.org/10.1016/j.jmmm.2016.01.079

[40] Ł. Dubiel, I. Stefaniuk, A. Wal, The Low-Field Microwave Absorption in EMR Spectra for $Ni_{50-x}Co_xMn_{35.5}In_{14.5}$ Ribbons. Materials, 15(17), (2022) 6016.https://doi.org/10.3390/ma15176016

[41] Z. Zhan, Z. Hu, K. Meng, J. Zhao, J. Chu, Temperature dependent phonon Raman scattering of Heusler alloy $Co_2Mn_xFe_{1-x}Al$/GaAs films grown by molecular-beam epitaxy. RSC Advances, 2(26), (2012) 9899. https://doi.org/10.1039/C2RA21255B

[42] M. Zhai, S. Ye, Z. Xia, F. Liu, C. Qi, X. Shi, G. Wang, Local Lattice Distortion Effect on the Magnetic Ordering of the Heusler Alloy $Co_2FeAl_{0.5}Si_{0.5}$ Film. Journal of Supercond and Novel Magnetism, 27(8), (2014) 1861–1865. https://doi.org/10.1007/s10948-014-2526-z

[43] K. Bera, S. Mukherjee, M. Mukadam, S. Mondal, M.K. Firoz, G. Vaitheeswaran, A. Roy, S.M. Yusuf, Selective electronic excitations in nearly half-metallic Heusler alloy NiFeMnSn—A Raman spectroscopic study. Applied Physics Letters, 121(5), (2022) 052404.https://doi.org/10.1063/5.0097464

Authors Contribution Statement

T. Naaraayanan: Conceptualization, Sample synthesis, Data curation, Methodology, Investigation, Writing – Original draft preparation. Prakash Bongurala: Writing – Reviewing and Editing. M. Saroja: Writing – Reviewing and Editing. M. Venkatachalam: Writing – Reviewing and Editing, Supervision. All the authors read and approved the final version of the manuscript.

Funding

The authors declare that no funds, grants or any other support were received during the preparation of this manuscript.

Competing Interests

The authors declare that there are no conflicts of interest regarding the publication of this manuscript.

Data Availability

The data supporting the findings of this study can be obtained from the corresponding author upon reasonable request.

Has this article screened for similarity?

Yes

About the License